ISSN 1069-3513, Izvestiya, Physics of the Solid Earth, 2007, Vol. 43, No. 1, pp. 13–23. © Pleiades Publishing, Ltd., 2007.

Damage Evolution and Fluid Flow in Poroelastic Rock[1]

V. Lyakhovsky[a] and Ya. Hamiel[a,b]

[a] *Geological Survey of Israel, 30 Malkhei Israel St., Jerusalem, 95501 Israel*

[b] *IGPP, Scripps Institution of Oceanography, University of California, San Diego, 9500 Gilman Dr., La Jolla, CA 92093, USA*

e-mail: vladi@geos.gsi.gov.il

Received June 8, 2006

Abstract—We present a formulation for mechanical modeling of the interaction between fracture and fluid flow. Our model combines the classic Biot poroelastic theory and a damage rheology model. The model provides an internally consistent framework for simulating coupled evolution of fractures and fluid flow together with gradual transition from brittle fracture to cataclastic flow in high-porosity rocks. The theoretical analysis, based on thermodynamic principles, leads to a system of coupled kinetic equations for the evolution of damage and porosity. A significant advantage of the model is the ability to reproduce the entire yield curve, including positive and negative slopes, in high-porosity rocks by a unified formulation. A transition from positive to negative values in the yield curve, referred to as a yield cap, is determined by the competition between the two thermodynamic forces associated with damage and porosity evolution. Numerical simulations of triaxial compression tests reproduce the gradual transition from localized brittle failure to distributed cataclastic flow with increasing pressure in high-porosity rocks and fit well experimentally measured yield stress for Berea sandstone samples. We modified a widely used permeability porosity relation by accounting for the effect of damage intensity on the connectivity. The new damage–permeability relation, together with the coupled kinetics of damage and porosity evolution, reproduces a wide range of realistic features of rock behavior. We constrain the model variables by comparisons of the theoretical predictions with laboratory results reporting porosity and permeability variation in rock samples during isotropic and anisotropic loading. The new damage–porosity–permeability relation enables simulation of coupled evolution of fractures and fluid flow and provides a possible explanation for permeability measurements in high-porosity rocks, referred to as the "apparent permeability paradox."

PACS numbers: 91.32.De; 91.32.Ik

DOI: 10.1134/S106935130701003X

1. INTRODUCTION

The coupled evolution of damage and porosity in porous rocks is fundamental to a variety of practical geological problems, including fluid flow in fractured sedimentary basins, nucleation of deformation features, the effective strength of the faulted crust, and the role of pore fluid pressure in earthquake failure and dike propagation. Previous studies have shed light on particular aspects of these geological problems and a certain coupling between them [Aydin and Johnson, 1978, 1983; Rice, 1992; Rubin, 1993; Wong and Zhu, 1999]. Further progress in this direction depends on researchers' ability to incorporate various aspects of rock deformation. A thermodynamically based continuum mechanics approach enables researchers to explicitly include the physics of fracture growth and facilitates better understanding of the effect of fracture growth mechanisms on the connectivity and flow characteristics of fracture systems.

In this paper, we present results of modeling the mechanical interaction of porous rock with pore-filling fluids, with a focus on understanding the fundamental processes that control relations between damage evolution during localization to fault zones and fluid flow characteristics.

1.1. Porous Rock Deformation

The fracture process in low-porosity crystalline rocks is associated with sharp localization of microfracturing into a narrow fault zone (e.g., [Lockner et al., 1992]) and with a monotonic increase in the yield stress under increasing confining pressure. The fracture process in high-porosity rocks is considerably more complex, featuring different modes of failure ranging from brittle failure to cataclastic flow [Wong et al., 1997]. The mode of failure of high-porosity rocks strongly depends on the confining pressure. At low pressures, failure is associated with nucleation and dilation of microcracks and the rock fails along a localized deformation zone [Lockner et al., 1992; Wong et al., 1997]. With an increase in the confining pressure, rather than microcracks being dilated, shear bands are dominated by porosity loss due to compaction and grain crushing [Menendez et al., 1996; Wong et al., 1997]. The band material becomes mechanically stron-

[1] The text was submitted by the authors in English.

ger than the surrounding host rock, leading to a locking of developed bands and migration of the deformation. Therefore, a further increase in loading leads to the sequential development of a relatively wide shear zone. Such shear zones often contain sets of narrow shear bands and are widely observed in the field as well as in the laboratory (e.g., [Aydin and Johnson, 1978; Mair et al., 2000]). Under high pressures, failure is accompanied by bulk sample compaction and a transition to nonlocalized cataclastic flow [Wong et al., 1997; Wong and Zhu, 1999]. The yield stress of high-porosity rocks at low pressures increases with pressure (a positive slope of the yield curve) until it achieves its maximal value at intermediate pressures. At relatively high pressures, the yield stress decreases with pressure (a negative slope of the yield curve). This transition from positive to negative values of the slope is related to the different modes of failure in high-porosity rocks, i.e., the transition from brittle failure to cataclastic flow [Wong et al., 1997].

Failure in porous rocks affects not only the distribution of damage and the local mechanical properties, but also the fluid flow and the permeability of fractured systems. A fracture network is an important component of many subsurface aquifers. Over the last three decades, numerous studies have shown that the flow and transport of fractured rocks are controlled by the geometry and connectivity of fractures (e.g., [Zhu et al., 1995; Renshaw, 1995, 1996; Bour and Davy, 1997; Seront et al., 1998]). Fractures of all scales in granite open and close in response to increases in pore pressure and tectonic stress and usually have a high connectivity even when the rock has been mechanically compressed [Brace et al., 1968]. In sedimentary rocks, a significant permeability reduction may result from compaction. The compaction or reduction in porosity is most generally modeled as a given function of the effective pressure or the difference between the confining pressure and the fluid pressure (e.g., [Fowler and Yang, 1999]). A compilation of laboratory data by David et al. [1994] shows that permeability κ as a function of porosity ϕ can usually be fitted by an empirical power-law relation of the form

$$\kappa = \kappa_0(\phi/\phi_0)^n, \quad (1)$$

where the power index n varies between 2 and 11 with a preferable value of $n \approx 3$ at high porosities. In addition to mechanical compaction, significant chemical compaction-controlled dissolution–precipitation and diffusive mass transfer may also lead to a reduction in rock porosity and affect the permeability (e.g., [Zhang et al., 1994; Olsen et al., 1998; Dijk and Berkowitz, 1998]). However, Tenthorey et al. [1998] reported a permeability reduction under constant porosity in a hot anisotropic loading test on quartz–feldspar sand. Moreover, Main et al. [2000] discussed an apparent paradox of a negative porosity–permeability correlation during shear-enhanced deformation in porous sandstone. A model that accounts for permeability change under constant porosity should explicitly include relations between permeability and pressure (e.g., [Rice, 1992; Wong and Zhu, 1999]) or relate permeability to a state variable representing rock fracture. The latest option for modeling of a permeability reduction caused by healing of microcracks is discussed in this paper.

1.2. Rheological Modeling of Poroelastic and Faulting Processes

Biot [1941] was the first to approach poroelastic media via thermodynamics. His now-classic theory supplements the elasticity equations for a poroelastic solid with a compressibility condition. A particularly useful case is the consolidation equation that relates the evolution of pore pressure to the stresses in a one-dimensional solid skeleton. Significant progress has been made in developing constitutive and field equations for linear poroelastic media (e.g., [Biot, 1955, 1956; Nikolaevski et al., 1970; Nur and Byerlee, 1971; Rice and Cleary, 1976; Rice, 1992; Detournay and Cheng, 1993]). A thermodynamic approach allows construction of nonlinear models for viscoelastoplastic porous media (e.g., [Biot, 1973; Coussy, 1995]).

A realistic rheological model of the faulting process should include subcritical crack growth from the very early stages of loading, material degradation due to increasing crack concentration, macroscopic brittle failure, postfailure deformation, and healing. Suitable variables should be defined to characterize the above aspects of deformation quantitatively in a framework compatible with continuum mechanics and thermodynamics. Among such approaches are Robinson's [1952] linear cumulative creep damage law, Hoff's [1953] ductile creep rupture theory, Kachanov's [1958, 1986] brittle rupture theory, Rabotnov's [1959, 1988] coupled damage creep theory, and many modifications of these theories.

Continuum damage mechanics uses the approach of irreversible thermodynamics [Onsager, 1931; Prigogine, 1955; deGroot and Mazur, 1962]. This approach was successfully applied to kinetics of chemical reactions and phase transitions (e.g., [Fitts, 1962; deGroot and Mazur, 1962]) and was used as a basis for variational methods of modeling continuous media (e.g., [Sedov, 1968; Malvern, 1969]). Following this framework, Mosolov and Myasnikov [1965] formulated a variational model of viscoplastic media (see also [Ekland and Temam, 1976]). Lyakhovsky and Myasnikov [1985] used the balance equations of energy and entropy to establish a thermodynamic foundation for a rheological model of damaged material [Myasnikov et al., 1990; Lyakhovsky et al., 1993, 1997a]. Lyakhovsky and Myasnikov [1984, 1985] and Lyakhovsky et al. [1997a, 1997b] developed a scalar damage model that accounts for nonlinear elasticity by adding to the free energy function of an elastic solid an additional second-order term and connected the evolving elastic moduli to a single damage variable. Hamiel et al.

[2004a, 2005a] generalized the framework to a viscoelastic damage model with a power-law relation between the damage variable and the effective elastic properties and provided additional experimental verification of the model. A similar approach was also used as the basis of other damage models (e.g., [Valanis, 1990; Papa, 1993; Hansen and Schreyer, 1994; Kachanov, 1994; Krajcinovic, 1996; Allix and Hild, 2002]). Fiber bundle models of damage [Newman and Phoenix, 2001; Turcotte et al., 2003] have similar ideas, with torn fibers corresponding to cracks. Frictional frameworks have an analogous physical concept phrased in terms of the contact area. This allowed Lyakhovsky et al. [2005] to develop quantitative connections between the observed phenomenology of the RS friction and the damage rheology model of Lyakhovsky et al. [1997a] and Hamiel et al. [2004b]. Hamiel et al. [2004a, 2005a] combined the damage rheology model with Biot's poroelastic theory to describe coupled evolution of damage, porosity, and fluid flow in porous rocks.

2. POROELASTIC DAMAGE MODEL

2.1. General Thermodynamic Relations

In this section, we briefly summarize the main features of the poroelastic damage model (for the detailed derivation of the governing equations, see [Hamiel et al., 2004a, 2005a]). Following Biot's theory of poroelasticity [Biot, 1941] and damage rheology theory (e.g., [Lyakhovsky et al., 1997a]), the free energy of a unit volume of a poroelastic solid F is a function of its state variables,

$$F = F(T, \varepsilon_{ij}, \zeta, \phi, \alpha), \tag{2}$$

temperature T, elastic strain tensor ε_{ij}, fluid volume content ζ, material porosity ϕ, and damage variable α. Since each variable can vary independently of the other variables, the Gibbs relation can be written as [Gibbs, 1961]

$$dF = -SdT + \frac{\partial F}{\partial \varepsilon_{ij}} d\varepsilon_{ij} + \frac{\partial F}{\partial \zeta} d\zeta + \frac{\partial F}{\partial \phi} d\phi + \frac{\partial F}{\partial \alpha} d\alpha, \tag{3}$$

where $S = -\dfrac{\partial F}{\partial T}$ is entropy density (Einstein's summation convention is assumed). The elastic strain tensor ε_{ij} is written as the difference between the total strain tensor $\varepsilon_{ij}^{\text{tot}}$ and the strain tensor describing the inelastic deformation $\varepsilon_{ij}^{\text{in}}$:

$$\varepsilon_{ij} = \varepsilon_{ij}^{\text{tot}} - \varepsilon_{ij}^{\text{in}}. \tag{4}$$

The equation for mass conservation of the fluid can be expressed as

$$\frac{d\zeta}{dt} + \nabla_i(q_i) = 0, \tag{5}$$

where q_i is the fluid flux with respect to the solid matrix.

The balance equations for the densities of the internal energy U and entropy S have the form (e.g., [Malvern, 1969; Coussy, 1995])

$$\frac{dU}{dt} = \frac{d}{dt}(F + TS) = -\rho_f \nabla_i(q_i h_f) + \sigma_{ij} e_{ij} - \nabla_i Q_i, \tag{6}$$

$$\frac{dS}{dt} = -\rho_f \nabla_i(q_i s_f) - \nabla_i\left(\frac{Q_i}{T}\right) + \frac{\Phi}{T}, \quad \Phi \geq 0, \tag{7}$$

where h_f is the enthalpy of a unit mass of the fluid, which is a function of the fluid entropy of a unit mass s_f and of the fluid pressure p ($dh_f = Tds_f + dp/\rho_f$), ρ_f is the fluid density; σ_{ij} is the stress tensor; Q_i is the heat flux; Φ is the local entropy production; and the strain rate tensor e_{ij} is a temporal derivative of the total strain tensor:

$$e_{ij} = \frac{d\varepsilon_{ij}^{\text{tot}}}{dt}. \tag{8}$$

Balance equations (6), (7) differ from the similar energy and entropy balance equations for elastic media with distributed damage [Lyakhovsky et al., 1997a] by the divergence term related to the energy and entropy advection due to pore fluid transport. The stress tensor and the fluid pressure are defined as [Malvern, 1969; Coussy, 1995]

$$\sigma_{ij} = \frac{\partial F}{\partial \varepsilon_{ij}}, \tag{9}$$

$$p = \frac{\partial F}{\partial \zeta}. \tag{10}$$

Substituting Gibbs relation (3) into energy and entropy balance equations (6), (7) and using fluid conservation (5) and the definitions of the stress tensor and the fluid pressure (9), (10), the local entropy production may be represented as

$$\Phi = -\frac{Q_i}{T}\nabla_i T + \sigma_{ij}\frac{d\varepsilon_{ij}^{\text{in}}}{dt} - q_i \nabla_i p - \frac{\partial F}{\partial \alpha}\frac{d\alpha}{dt} - \frac{\partial F}{\partial \phi}\frac{d\phi}{dt} \geq 0. \tag{11}$$

Each term in this equation represents entropy production due to a different physical process and can be classified according to its tensor rank. Thus, the first term of Eq. (11) describes entropy production by heat conduction; the second term is due to viscous dissipation; the third term is related to the fluid transport process; and the last two terms are related to internal energy changes caused by microcracking and inelastic porosity change, respectively. As a standard approach, we split terms of different tensor rank. Therefore, the viscous dissipation term is divided into volumetric and deviatoric parts. This separation is consistent with the distinction between shear and bulk viscosities [McKenzie, 1984]. The usual assumption of a plastically incom-

pressible matrix means that an irreversible change in the bulk volume is equal to an inelastic porosity change. Thus, the time derivative of the trace of the inelastic strain tensor $\varepsilon_{ij}^{\text{in}}$ is equal to the time derivative of the inelastic porosity, $\frac{d\phi}{dt} = -\frac{d\varepsilon_{kk}^{\text{in}}}{dt}$, and the scalar part of the entropy production (Φ_{scalar}) can be rewritten as $\left(\sigma_m = -\frac{1}{3}\sigma_{kk}\right)$

$$\Phi_{\text{scalar}} = \left(-\frac{\partial F}{\partial \alpha}\frac{d\alpha}{dt}\right) - \left(\frac{\partial F}{\partial \phi} + \sigma_m\right)\frac{d\phi}{dt} \geq 0. \qquad (12)$$

Close to equilibrium, a constitutive equation gives the thermodynamic flux as a linear function of the thermodynamic force for each dissipation [deGroot and Mazur, 1962; Malvern, 1969]. These phenomenological equations guarantee a nonnegative value of entropy production. Thus, we write the phenomenological equations for the kinetics of the internal state variables α and ϕ as a set of two coupled differential equations:

$$\begin{aligned} \frac{d\phi}{dt} &= C_{\phi\phi}\left(\frac{\partial F}{\partial \phi} + \sigma_m\right) + C_{\phi\alpha}\frac{\partial F}{\partial \alpha}, \\ \frac{d\alpha}{dt} &= C_{\alpha\phi}\left(\frac{\partial F}{\partial \phi} + \sigma_m\right) + C_{\alpha\alpha}\frac{\partial F}{\partial \alpha}, \end{aligned} \qquad (13)$$

where the matrix of the kinetic coefficients C has to satisfy conditions discussed by deGroot and Mazur [1962] and Malvern [1969]. Hamiel et al. [2004a] showed that the interaction between evolving material damage and porosity change including a gradual transition from brittle failure to cataclastic flow is obtained if the matrix of kinetic coefficients is antisymmetric. In this case, the conditions for nonnegative entropy production are reduced to

$$C_{\phi\phi} \leq 0, \quad C_{\alpha\alpha} \leq 0, \quad C_{\phi\alpha} = -C_{\alpha\phi}. \qquad (14)$$

2.2. Equation of State and Kinetic Coefficients

An expression for the free energy of a damaged poroelastic medium should account for the nonlinear elastic properties and the coupling term of the saturated medium. Combining Biot's coupling term [Biot, 1941, 1956] with the free energy for nonlinear damaged media [Lyakhovsky et al., 1997a], Hamiel et al. [2004a] suggested the following energy equation:

$$\begin{aligned} F = \frac{\lambda(\alpha, \phi)}{2} I_1^2 + \mu(\alpha, \phi) I_2 - \gamma(\alpha, \phi) I_1 \sqrt{I_2} \\ + \frac{1}{2} M[\beta I_1 - (\zeta - \phi)]^2. \end{aligned} \qquad (15)$$

The poroelastic energy (15) includes two Hookean terms with the Lamé drained moduli λ, μ ($I_1 = \varepsilon_{kk}$; $I_2 = \varepsilon_{ij}\varepsilon_{ij}$) and an additional nonlinear term with the strain coupling modulus γ. M and β are the Biot modulus and Biot's coefficient for porous media, respectively. Hamiel et al. [2005b] demonstrated that expressions for the stress tensor and fluid pressure (9), (10) derived using energy potential (15) enable proper description of the rock dilation and related variation in fluid pressure as a function of shear stress that is widely observed in rock mechanics experiments. The effect of rock degradation is simulated by making the poroelastic moduli functions of the damage variable and porosity. According to damage mechanics, the change in the damage variable is directly related to the change in the rigidity of the rock. For mathematical simplicity with the lack of experimental data, Agnon and Lyakhovsky [1995] assumed that the moduli μ and γ are linear functions of α and the modulus λ is constant. With this assumption, the onset of positive damage evolution occurs at the critical strain invariant ratio ξ_0, the parameter that separates states of deformation involving material degradation and healing. Agnon and Lyakhovsky [1995] and Lyakhovsky et al. [1997a] related this parameter to the angle of internal friction by considering the critical shear stress for Mohr–Coulomb sliding. This model formulation does not account for possible stable weakening, and once the strain field exceeds ξ_0, unstable weakening of the sample occurs. Hamiel et al. [2004b, 2006] showed that power-law relations between the damage variable and elastic moduli can improve fitting of the damage rheology model predictions to experimental data, but linear relations are still a good approximation.

Hamiel et al. [2004a] suggested that microcracks do not directly change the poroelastic coupling term in Eq. (15) and, thus, the Biot modulus M and the Biot coefficient β do not depend on the damage parameter. On the other hand, the poroelastic moduli decrease with an increase in porosity (e.g., [Dvorkin et al., 1994; Mavko and Mukerji, 1995]). If the porosity is regarded as the concentration of roughly spherical inclusions in the elastic matrix, the macroscopic properties of the bulk are expected to decrease linearly with increasing ϕ (e.g., [Christensen, 1979]). This linear relation is the first-order approximation to more general models for the effective moduli and their dependence on porosity in poroelastic media (e.g., [Dvorkin et al., 1994; Mavko and Mukerji, 1995; Hudson, 2000]). This linear approximation is also supported by experiments on sandstone reported by Dvorkin and Nur [1996]. Hence, the elastic moduli are assumed to be proportional to the term $(1 - \phi/\phi_{\text{cr}})$, where ϕ_{cr} is the porosity upper bound at which the material loses its stiffness. Finally, the effective poroelastic moduli can be written as

$$\lambda = \lambda_0\left(1 - \frac{\phi}{\phi_{\text{cr}}}\right),$$

$$\mu = \left(1 - \frac{\phi}{\phi_{cr}}\right)(\mu_0 + \xi_0\gamma_1\alpha),$$
$$\gamma = \left(1 - \frac{\phi}{\phi_{cr}}\right)\gamma_1\alpha, \quad (16)$$
$$M = M_0\left(1 - \frac{\phi}{\phi_{cr}}\right),$$

where μ_0, γ_1, and ξ_0 are constants for each material. The coefficient ξ_0 is related to the friction angle [Agnon and Lyakhovsky, 1995], and the moduli μ_0, γ_1 are constrained by the conditions for loss of convexity (Eqs. (14), (15) in [Lyakhovsky et al., 1997]). We also adopt Terzaghi's assumption ($\beta = 1$) as a useful approximation (see the discussion in [Nur and Byerlee, 1971]). The effective stress then becomes the sum of the total stress and the fluid pressure. The model equations reduce to the equations of state developed by Biot [1941, 1956] for linear poroelastic media in the limit of zero damage intensity ($\alpha = 0$). At the same time, these equations reduce to the stress–strain relations derived by Lyakhovsky et al. [1997a] for damaged elastic media with vanishing fluid pressure ($p = 0$).

Using energy potential (15) and expressions (16) for the poroelastic moduli, kinetic equations (13) can be rewritten as

$$\frac{d\phi}{dt} = -C_{\phi\phi}P_e + C_{\alpha\phi}\gamma_1 I_2(\xi - \xi_0), \quad (17a)$$

$$\frac{d\alpha}{dt} = C_{\alpha\phi}P_e + C_{\alpha\alpha}\gamma_1 I_2(\xi - \xi_0). \quad (17b)$$

We also use the asymmetry of the matrix of the positive kinetic coefficients (14) and introduce the effective pressure, equal to the mean stress minus the fluid pressure $\left(P_e = -\frac{\sigma_{kk}}{3} - p\right)$. Each term in kinetic equations (17) represents the thermodynamic forces related to damage ($\partial F/\partial\alpha$) and to porosity change (P_e). The terms with the kinetic coefficients $C_{\alpha\alpha}$ and $C_{\phi\phi}$ are responsible for the evolution of α and ϕ as functions of damage- and porosity-related forces, respectively. The coefficient $C_{\alpha\phi}$ is responsible for the coupling between the kinetics of damage and porosity. Hamiel et al. [2004a] showed that $C_{\phi\phi}$ is of the order of 10^{-18}–10^{-22} $(\text{Pa s})^{-1}$ and therefore is negligibly small for the laboratory time scale. Lyakhovsky et al. [1997] and Hamiel et al. [2004b] used results of laboratory experiments to constrain the damage rate coefficient $C_{\alpha\alpha}$. They found that $C_{\alpha\alpha}$ on the order of $0.5/\gamma_1$ to $10/\gamma_1$ $(\text{Pa s})^{-1}$ provided a good fit to observed data for damage increase.

Following the Hertzian contact theory, Hamiel et al. [2004a] suggested that $C_{\alpha\phi}$ is a power-law expression of the effective pressure, $C_{\alpha\phi} = D(\phi)P_e^n$. They demonstrated that a transition from positive to negative values of the slope of the yield curve (a yield cap) is a general feature of the model for $n > 1$ and estimated $D \sim 10^{-10}$ MPa^{-3} s^{-1} and $n = 2$ for Berea sandstone with $\phi \sim 20\%$. The kinetic coefficient $D(\phi)$ decreases with decreased porosity and becomes negligibly small for crystalline rocks. Hence, for low-porosity, crystalline rocks, the condition for the onset of damage is $\xi = \xi_0$, corresponding to the straight line in Fig. 1. For porous rocks, this line separates the region with material degradation ($d\alpha/dt > 0$) and dilation ($d\phi/dt > 0$) from the region with degradation and compaction. The yield curve corresponding to the onset of damage has the cap shape schematically shown in Fig. 1. Only below this curve do both healing ($d\alpha/dt < 0$) and compaction ($d\phi/dt < 0$) occur. Hamiel et al. [2004a] presented a detailed sensitivity analysis of the yield curve for different model coefficients.

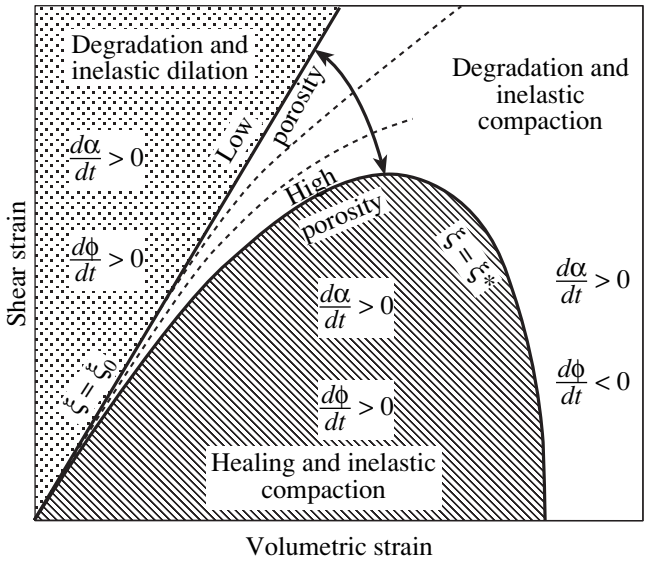

Fig. 1. Schematic diagram of the states of strains associated with different modes of material behavior.

Motivated by the observed logarithmic increase in the static coefficient of friction with time, Lyakhovsky et al. [1997a] used an exponential function for the kinetics of damage decrease (healing). The analytical and numerical results of Lyakhovsky et al. [2005] provide quantitative connections between the healing parameters of the damage rheology model and the parameters of rate- and state-dependent friction. Laboratory experiments [Olsen et al., 1998; Tenthorey et al., 2003] reveal a strong connection between material strengthening and grain crushing and compaction in high-porosity rocks. To account for this porosity-related enhancement of material healing, the kinetic coefficient $C_{\alpha\alpha}$ is rewritten as

$$C_{\alpha\alpha}(\alpha, \phi) = \begin{cases} \text{const} \ \text{ for } \ \dfrac{d\alpha}{dt} \geq 0 \\ A_1 \exp\left(\dfrac{\alpha}{A_2}\right) \exp(B(\phi_0 - \phi)) \ \text{ for } \ \dfrac{d\alpha}{dt} < 0, \end{cases} \quad (18)$$

where ϕ_0 is the initial porosity. Thus, the damage rate coefficient for material healing is now a function of both the damage variable and the material porosity. Material healing usually also leads to a reduction in permeability without a significant change in porosity. This feature was reported by Tenthorey et al. [1998], who measured permeability reduction in a hot anisotropic loading test on quartz–feldspar sand subjected to constant loads of 25 and 50 MPa (Fig. 2). The total porosity measured during the experiment remained constant. In the framework of our model, this permeability reduction may be related to the reduction of the damage variable (α). Therefore, we seek a new rule for permeability evolution that takes into account the variable level of damage and suggest a new modified equation accounting not only for the porosity–permeability but also for the porosity–damage relation:

$$\kappa = \kappa_0(\phi/\phi_0)^n(\alpha/\alpha_0)^m. \quad (19)$$

Comparing the numerical solution for the damage recovery under constant load conditions corresponding to the experiments of Tenthorey et al. [1998] with the measured permeability reduction, enabling us to gain constraints on the exponential value m in (19), a good fit between the measured permeability reduction and the numerical solution is obtained for $m = 2$ (Fig. 2). This value, together with $n = 3$ for the permeability–porosity relation, is used for estimation of the evolving permeability in the simulations presented in the following section.

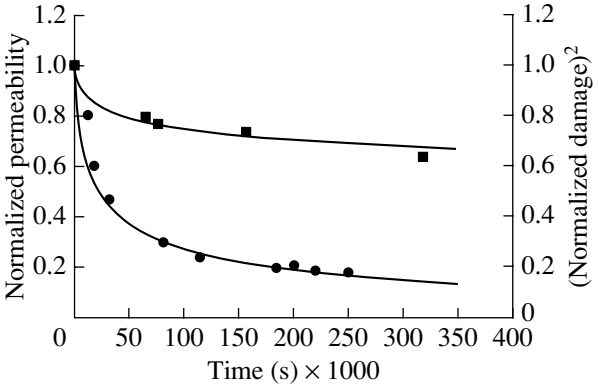

Fig. 2. Normalized permeability (k) evolution at constant porosity ($\phi = \phi_0$) from Tenthorey et al. [1998] compared with the normalized square of damage variable (α) evolution for a constant load of 25 (squares) and 50 (circles) MPa. As shown in the figure, there is good agreement between the data and the permeability calculated using Eq. (19) with $m = 2$.

3. NUMERICAL SIMULATIONS

We present a numerical simulation of standard triaxial rock mechanics tests with high-porosity samples. The model equations are solved using an explicit-in-time scheme following the Fast Lagrangian Analysis of Continua (FLAC) algorithm [Cundall and Board, 1988; Cundall, 1989; Poliakov et al., 1993; Lyakhovsky et al., 2001] modified by [Hamiel et al., 2005a] for evolving damage and porosity. Simulations are run with constant confining pressures starting from 25 up to 400 MPa and a strain rate of 5×10^{-5} s^{-1}. The sample has a rectangular shape with an aspect ratio of 1 : 2 between the horizontal and vertical sizes. In these simulations, we used the following mechanical properties of the rock: $\lambda = 7 \times 10^3$ MPa; $\mu_0 = 1.8 \times 10^4$ MPa; $\xi_0 = -0.8$, corresponding to an internal friction angle $\varphi = 65°$; the Biot modulus $M = 1.5 \times 10^4$ MPa; the Biot coefficient $\beta = 1$; and an initial porosity $\phi_0 = 20\%$, corresponding to the properties of Berea sandstone measured in laboratory experiments [Lockner et al., 1992]. A small, initially random distribution of damage ($\alpha < 0.1$) reproduces initial heterogeneity of a sample. A constant fluid pressure of $p = 5$ MPa was set along all of the boundaries to mimic drained conditions. In order to avoid boundary effects, a thin undamaged layer with constant porosity (20%) was set at the top and bottom boundaries of the sample. The set of simulations allows investigation of the model behavior under various pressures and reproduction of the transition from brittle failure to cataclastic flow

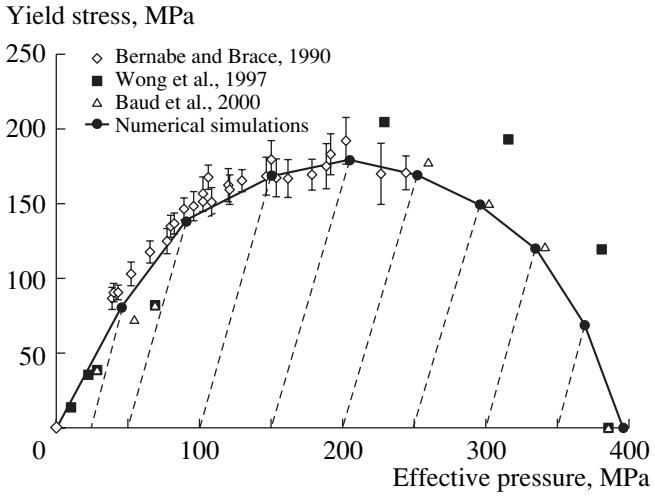

Fig. 3. Experimentally measured yield stress for Berea sandstone compared with the calculated curve from the numerical simulations. Symbols indicate experimental results from [Bernabe and Brace, 1990; Wong et al., 1997; Baud et al., 2000]. The dashed lines indicate the numerical loading path from the beginning of the modeling with zero differential stress up to the yield stress. The black circles indicate the yield stress from the numerical simulations.

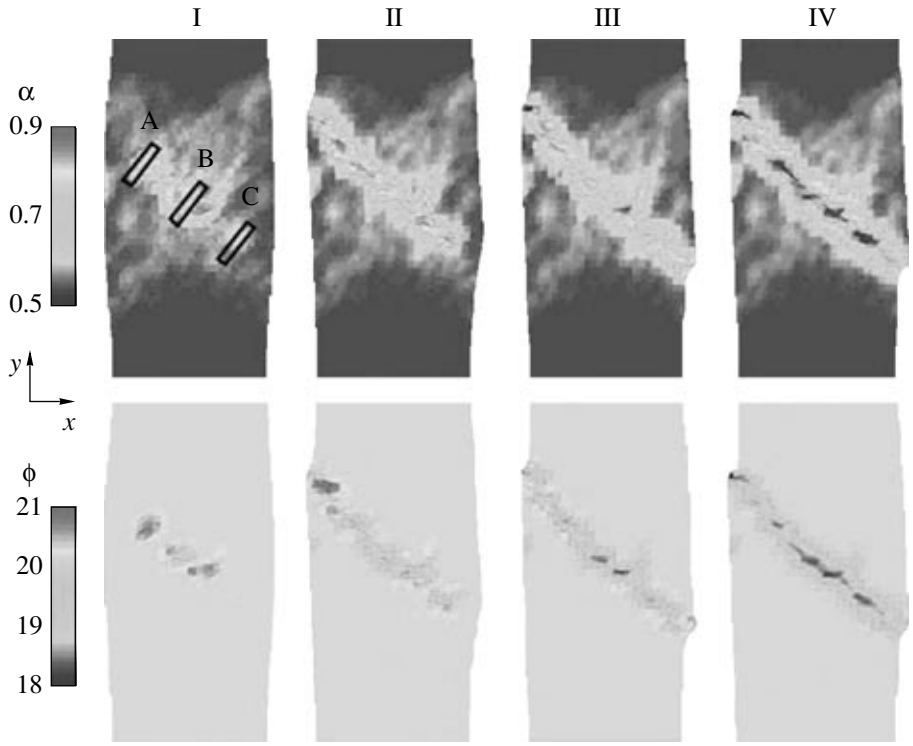

Fig. 4. Four snapshots representing four stages of rock sample deformation during triaxial test simulation with 50 MPa confining pressure and 20% initial porosity. Each stage is represented by the damage variable (α) distribution (upper snapshots) and the porosity (ϕ) distribution (lower snapshots). Rectangles A, B, and C represent the areas in which the permeability was calculated and presented in Fig. 5.

anticipated from the analysis of Hamiel et al. [2004a]. The numerical simulations further allow visualization of the transition from localized to nonlocalized damage and porosity distributions. Yielding (occasionally termed first yielding) in our model is related to the onset of an increase in damage. This relation is in agreement with experimental observations on a rapid increase in acoustic emission after the yield stress is exceeded [Zhang et al., 1990; Wong et al., 1997]. Figure 3 shows the yield stress calculated from the numerical simulations. The shape of the calculated yield curve is determined by the competition between the first and second terms in the equation for damage evolution (17b). For low effective pressures, the second term is dominant, causing a positive slope of the curve, whereas, for high effective pressures, the first term becomes dominant, causing a negative slope. Also shown in Fig. 3 are the experimentally measured yield stresses for Berea sandstone from Bernabe and Brace [1990], Wong et al. [1997], and Baud et al. [2000]. The measured values of yield stress for Berea sandstone samples under high confining pressures show a significant scatter between data sets reported by different authors. Therefore, the calculated yield curve cannot fit all the presented data sets simultaneously. The calculated yield curve provides a reasonable fit to the experimentally measured yield stress for Berea sandstone at high pressures reported by Baud et al. [2000]. The experimental data under high pressures reported by Wong et al. [1997] could also be fitted with the present model with a higher value of the kinetic coefficient $C_{\alpha\phi}$ (not shown here).

The simulated transition from brittle failure to cataclastic flow is controlled by a confining pressure similar to laboratory experimental results. Figure 4 presents results for the damage and porosity distribution during simulation with a relatively low (50 MPa) confining pressure with localized deformation and a small barreling effect. The four snapshots correspond to different stages of the fracture zone evolution: (I) nucleation, (II) in-plane propagation, (III) total failure, and (IV) sliding and out-of-plane growth. Figure 5 presents the width of the deformation zone normalized to the sample length that refers to the region whose initial porosity of 20% is reduced by more than 1%. The change in permeability during simulation with a relatively low (50 MPa) confining pressure is presented in Figure 5. The permeability change was calculated using Eq. (19) for three different regions A, B, and C as shown in Fig. 4. Slight compaction of the whole sample at the initial stage of loading before the onset of damage leads to a minor permeability reduction at this stage (Fig. 5). During the nucleation stage, the fracture zone is dilated and the inelastic porosity increases (Fig. 4, stage I). The permeability in the selected regions quickly increases by a factor of 2 or even more (Fig. 5),

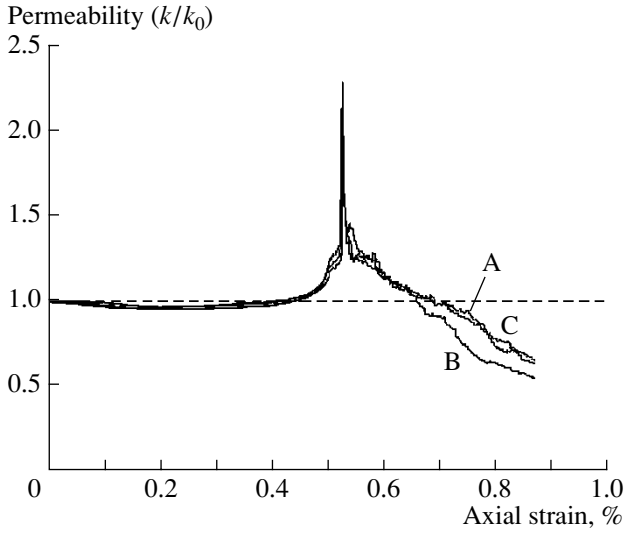

Fig. 5. Normalized width of a deformation zone versus axial strain (heavy line). A deformation zone refers to a zone in which the initial porosity of 20% is reduced by more than 1%. Permeability change due to damage and porosity evolution (Eq. (19)) for three different regions of the simulated sample (thin lines marked A, B, and C). See Fig. 4 for the location of regions A, B, and C.

but no deformation zone is formed yet (Fig. 5). During the next stages, the compaction of a newly created damage zone leads to porosity-enhanced healing (Eq. (18)), fast creation of a wide deformation zone (Fig. 5), and a significant reduction in permeability to values below its initial level (Fig. 5). The strengthening of the compacted rock inside the deformation zone leads to an increase in damage outside the deformation zone and to the progressive development of a wide deformation zone (Fig. 5). This model prediction of the evolution of the deformation zone is in agreement with observations from experiments on sandstone samples [Bernabe and Brace, 1990; Mair et al., 2000; Besuelle, 2001]. The porosity reduction within the deformation zone, together with its widening, leads to a gradual decrease in permeability in the selected regions. The permeability increase at the stage of fault nucleation followed by the gradual permeability reduction associated with growth of the deformation qualitatively reproduces the measured permeability in porous sandstone samples, referred to as the "apparent permeability paradox" (e.g., [Main et al., 2000; Ngwenya et al., 2003]).

4. DISCUSSION AND CONCLUSIONS

We have presented a thermodynamically based formulation of the poroelastic damage model that provides a generalization of Hookean elasticity and Biot poroelasticity to a nonlinear continuum mechanics framework. In agreement with theoretical analysis of the thermodynamic forces related to porosity and damage variation, the numerical model reproduces different modes of macroscopic failure for high-porosity rocks. The competition between these forces reproduces the transition from brittle failure to cataclastic flow in porous rocks. From a micromechanical point of view, rock deformation is associated with the formation and growth of internal flaws. These flaws can be divided into two classes: microcracks (damage) in the matrix of the porous rock, acting as high stress concentrators and hence leading to brittle failure, and pores, acting to dissipate stress concentrations and hence leading to distributed flow. The approach presented is based on the assumption that the density of microcracks is uniform over a length scale much larger than the length of a typical crack, yet much smaller than the size of the entire deforming domain. For a system with a sufficiently large number of cracks and pores, one can define a representative volume in which the flaw density is uniform and introduce an intensive damage variable and porosity for this volume.

The numerical simulations presented confirm theoretical predictions and allow calibration of the poroelastic damage model. In agreement with theoretical analysis of the thermodynamic forces related to porosity change and damage accumulation, the numerical model reproduces different modes of macroscopic failure for high-porosity rocks from brittle failure at relatively low confining pressures to cataclastic flow at relatively high confining pressures. We analyzed the permeability evolution (Fig. 5) during a simulation with a relatively low confining pressure (50 MPa). In this simulation, during the nucleation stage of a fault zone, the fracture zone is dilated and the porosity increases, leading to permeability enhancement. At the later stages, a widening deformation zone with significantly reduced porosity is created, leading to a gradual permeability reduction. This mechanism explains the reported permeability measurements in porous rocks, referred to as the "apparent permeability paradox" (e.g., [Main et al., 2000; Ngwenya et al., 2003]). Our permeability–porosity–damage relation (19) has the same characteristic behavior as the measured permeability in tests with relatively low confining pressures (up to 100 MPa [e.g., Main et al., 2000; Ngwenya et al., 2003; Tenthorey et al., 2003]). Further corroboration of this relation should include a comparison between permeabilities predicted by the model and measured during triaxial tests at relatively high confining pressures.

The developed model provides an internally consistent framework for simulating gradual transition from brittle fracture to cataclastic flow in high-porosity rocks and coupled evolution of fractures and fluid flow in a variety of practical geological and engineering problems such as earthquakes, nucleation of deformation features, and fluid flow during seismic cycles.

ACKNOWLEDGMENTS

We acknowledge support from the Israel Science Foundation, grant no. ISF 479/03.

REFERENCES

1. A. Agnon and V. Lyakhovsky, "Damage Distribution and Localization during Dyke Intrusion," in *The Physics and Chemistry of Dykes*, Ed. by G. Baer and A. Heimann (Balkema, Rotterdam, 1995), pp. 65–78.
2. O. Allix and F. Hild, *Continuum Damage Mechanics of Materials and Structures* (Elsevier, Amsterdam, 2002).
3. A. Aydin and A. M. Johnson, "Development of Faults as Zones of Deformation Bands and as Slip Surfaces in Sandstone," Pure Appl. Geophys. **116**, 931–942 (1978).
4. A. Aydin and A. M. Johnson, "Analysis of Faulting in Porous Sandstones," J. Struct. Geol. **5**, 19–31 (1983).
5. P. Baud, W. Zhu, and T.-F. Wong, "Failure Mode and Weakening Effect of Water on Sandstone," J. Geophys. Res. **105**, 16371–16389 (2000).
6. Y. Bernabe and W. F. Brace, "Deformation and Fracture of Berea Sandstone," in *The Brittle–Ductile Transition in Rocks (Geophys. Monogr., 56)*, Ed. by A. G. Duba, W. B. Durham, J. W. Handin, and H. F. Wang (AGU, Washington, 1990), pp. 91–101.
7. P. Besuelle, "Compacting and Dilating Shear Bands in Porous Rock: Theoretical and Experimental Conditions," J. Geophys. Res. **106**, 13 435–13 442 (2001).
8. M. A. Biot, "General Theory of Three-Dimensional Consolidation," J. Appl. Phys. **12**, 155–164 (1941).
9. M. A. Biot, "Theory of Elasticity and Consolidation for a Porous Anisotropic Solid," J. Appl. Phys. **26**, 182–185 (1955).
10. M. A. Biot, "General Solutions of the Equations of Elasticity and Consolidation for a Porous Material," J. Appl. Mech. **78**, 91–96 (1956).
11. M. A. Biot, "Nonlinear and Semilinear Rheology of Porous Solids," J. Geophys. Res. **78**, 4924–4937 (1973).
12. O. Bour and P. Davy, "Connectivity of Random Fault Network Following a Power Law Fault Length Distribution," Water Res. Res. **33**, 1567–1583 (1997).
13. W. F. Brace, J. B. Walsh, and W. T. Frangos, "Permeability of Granite under High Pressure," J. Geophys. Res. **73**, 2225–2236 (1968).
14. R. M. Christensen, *Mechanics of Composite Materials* (Wiley-Intersci., New York, 1979).
15. O. Coussy, *Mechanics of Porous Continua* (Wiley, Chichester, 1995).
16. P. A. Cundall, "Numerical Experiments on Localization in Frictional Materials," Ign. Arch. **59**, 148–159 (1989).
17. P. A. Cundall and M. Board, "A Microcomputer Program for Modeling Large-Strain Plasticity Problems," in *Proc. 6th Int. Conf. Numerical Methods in Geomechanics, Innsbruck*, Ed. by C. Swoboda (Balkema, Rotterdam, 1988), pp. 2101–2108.
18. C. David, T.-F. Wong, W. Zhu, and J. Zang, "Laboratory Measurements of Compaction-Induced Permeability Change in Porous Rocks: Implications for the Generation and Maintenance of Pore Pressure Excess in the Crust," Pure Appl. Geophys. **143**, 425–456 (1994).
19. S. R. deGroot and P. Mazur, *Nonequilibrium Thermodynamics* (North-Holland, Amsterdam, 1962).
20. E. Detournay and A. H.-D. Cheng, "Fundamentals of Poroelasticity," in *Comprehensive Rock Engineering: Principles, Practice and Projects*, Vol. II: *Analysis and Design Methods*, Ed. by C. Fairhurst (Pergamon, 1993), pp. 113–171.
21. P. Dijk and B. Berkowitz, "Precipitation and Dissolution of Reactive Solutes in Fractures," Water Res. Res. **34**, 457–470 (1998).
22. J. Dvorkin, A. Nur, and H. Yin, "Effective Properties of Cemented Granular Materials," Mech. Mater. **18**, 351–366 (1994).
23. J. Dvorkin and A. Nur, "Elasticity of High-Porosity Sandstones: Theory for Two North Sea Data Sets," Geophysics **61**, 1363–1370 (1996).
24. I. Ekland and R. Temam, *Convex Analysis and Variational Problems* (Elsevier, Amsterdam, 1976).
25. A. C. Fowler and X. Yang, "Pressure Solution and Viscous Compaction in Sedimentary Basins," J. Geophys. Res. **104**, 12 989–12 997 (1999).
26. J. W. Gibbs, *The Scientific Papers*, Vol. 1: *Thermodynamics* (New York, 1961).
27. Y. Hamiel, V. Lyakhovsky, and A. Agnon, "Coupled Evolution of Damage and Porosity in Poroelastic Media: Theory and Applications to Deformation of Porous Rocks," Geophys. J. Int. **156**, 701–713 (2004a).
28. Y. Hamiel, Y. Liu, V. Lyakhovsky, et al., "A Visco-Elastic Damage Model with Applications to Stable and Unstable Fracturing," Geophys. J. Int. **159**, 1155–1165 (2004b).
29. Y. Hamiel, V. Lyakhovsky, and A. Agnon, "Poroelastic Damage Rheology: Dilation, Compaction, and Failure of Rocks," Geochem. Geophys. Geosyst., No. 6, Q01008 (2005a).
30. Y. Hamiel, V. Lyakhovsky, and A. Agnon, "Rock Dilation, Nonlinear Deformation, and Pore Pressure Change under Shear," Earth Planet. Sci. Lett. **237**, 577–589 (2005b).
31. Y. Hamiel, O. Katz, V. Lyakhovsky, et al., "Stable and Unstable Damage Evolution in Rocks with Implications to Fracturing of Granite," Geophys. J. Int. (2006) (in press).
32. N. R. Hansen and H. L. Schreyer, "A Thermodynamically Consistent Framework for Theories of Elastoplasticity Coupled with Damage," Int. J. Solids Structures **31**, 359–389 (1994).
33. N. J. Hoff, "The Necking and Rupture of Rods Subjected to Constant Tensile Loads," J. Apl. Mech **20**, 105–108 (1953).
34. J. A. Hudson, "The Effect of Fluid Pressure on Wave Speeds in a Cracked Solid," Geophys. J. Int. **143**, 302–310 (2000).
35. L. M. Kachanov, "On the Time to Rupture under Creep Conditions," Izv. Acad. Nauk SSSR, Otdel. Tekhn. Nauk, No. 8, 26–31 (1958).
36. L. M. Kachanov, *Introduction to Continuum Damage Mechanics* (Martinus Nijhoff, 1986).
37. M. Kachanov, "On the Concept of Damage in Creep and in the Brittle–Elastic Range," Int. J. Damage Mech. **3**, 329–337 (1994).

38. D. Krajcinovic, *Damage Mechanics* (Elsevier, Amsterdam, 1996).

39. D. A. Lockner, J. D. Byerlee, V. Kuksenko, et al., "Observations of Quasi-Static Fault Growth from Acoustic Emissions," *Fault Mechanics and Transport Properties of Rocks (Int. Geophys. Series, Vol. 51),* Ed. by B. Evans and T.-F. Wong (Academic, San Diego, CA, 1992), pp. 3–31.

40. V. A. Lyakhovsky and V. P. Myasnikov, "On the Behavior of an Elastic Cracked Solid," Izv. Akad. Nauk SSSR, Fiz. Zemli **10**, 71–75 (1984).

41. V. A. Lyakhovsky and V. P. Myasnikov, "On the Behavior of a Visco-Elastic Cracked Solid," Izv. Akad. Nauk SSSR, Fiz. Zemli, No. 4, 28–35 (1985).

42. V. Lyakhovsky, Y. Podladchikov, and A. Poliakov, "Rheological Model of a Fractured Solid," Tectonophysics **226**, 187–198 (1993).

43. V. Lyakhovsky, Y. Ben-Zion, and A. Agnon, "Distributed Damage, Faulting, and Friction," J. Geophys. Res. **102**, 27 635–27 649 (1997a).

44. V. Lyakhovsky, Z. Reches, R. Weinberger, and T. E. Scott, "Non-Linear Elastic Behavior of Damaged Rocks," Geophys. J. Int. **130**, 157–166 (1997b).

45. V. Lyakhovsky, A. Ilchev, and A. Agnon, "Modeling of Damage and Instabilities of Rock Mass by Means of a Non-Linear Rheological Model," in *Dynamic Rock Mass Response to Mining (Rock Bursts and Seismicity in Mines—RaSiM5)*, Ed. by G. Van Aswegen, R. J. Durrheim, and W. D. Ortlepp (South African Institute of Mining and Metallurgy, Johannesburg, 2001), pp. 413–420.

46. V. Lyakhovsky, Y. Ben-Zion, and A. Agnon, "A Visco-Elastic Damage Rheology and Rate- and State-Dependent Friction," Geophys. J. Int. **161**, 179 –190 (2005).

47. I. G. Main, O. Kwon, B. T. Ngwenya, and S. C. Elphick, "Fault Sealing during Deformation-Band Growth in Porous Sandstone," Geology **28**, 1131–1134 (2000).

48. K. Mair, I. Main, and S. Elphick, "Sequential Growth of Deformation Bands in the Laboratory," J. Struct. Geol **22**, 25–42 (2000).

49. L. E. Malvern, *Introduction to the Mechanics of a Continuum Medium* (Prentice-Hall, Englewood Cliffs, 1969).

50. G. Mavko and T. Mukerji, "Seismic Pore Space Compressibility and Gassmann's Relation," Geophysics **60**, 1743–1749 (1995).

51. P. Mazur, *Nonequilibrium Thermodynamics* (North-Holland, Amsterdam, 1962).

52. D. P. McKenzie, "The Generation and Compaction of Partially Molten Rock," J. Petrol. **25**, 713–765 (1984).

53. B. Menendez, W. Zhu, and T.-F. Wong, "Micromechanics of Brittle Faulting and Cataclastic Flow in Berea Sandstone," J. Struct. Geol. **18**, 1–16 (1996).

54. P. P. Mosolov and V. P. Myasnikov, "Variational Methods in Flow Theory of Visco-Plastic Media," Appl. Math. Mech. **29**, 468–492 (1965).

55. V. P. Myasnikov, V. A. Lyakhovsky, and Yu. Yu. Podladchikov, "Non-Local Model of Strain-Dependent Visco-Elastic Media," Dokl. Akad. Nauk SSSR **312**, 302–305 (1990).

56. W. I. Newman and S. L. Phoenix, "Time-Dependent Fiber Bundles with Local Load Sharing," Phys. Rev. E **63** (2) (2001).

57. B. T. Ngwenya, O. Kwon, S. C. Elphick, and I. G. Main, "Permeability Evolution during Progressive Development of Deformation Bands in Porous Sandstones," J. Geophys. Res. **108** (B7), 2343 (2003).

58. V. N. Nikolaevskii, K. S. Vasniev, A. T. Gorbunov, and G. A. Zotov, *Mechanics of Saturated Porous Media* (Nedra, Moscow, 1970) [in Russian].

59. A. Nur and J. D. Byerlee, "An Exact Effective Stress Law for Elastic Deformation of Rock with Fluids," J. Geophy. Res. **76**, 6414–6419 (1971).

60. M. P. Olsen, C. H. Scholz, and A. Leger, "Healing and Sealing of a Simulated Fault Gouge under Hydrothermal Conditions: Implications for Fault Healing," J. Geophys. Res. **103**, 7421–7430 (1998).

61. L. Onsager, "Reciprocal Relations in Irreversible Processes," Phys. Rev. **37**, 405–416 (1931).

62. E. Papa, "A Damage Model for Concrete Subjected to Fatigue Loading," Eur. J. Mech., A/Solids **12**, 429–440 (1993).

63. A. Poliakov, P. Cundall, Y. Podladchikov, and V. Lyakhovsky, "An Explicit Inertial Method for the Simulation of Viscoelastic Flow: An Evaluation of Elastic Effects on Diapiric Flow in Two- and Three-Layer Model," in *Proc. NATO Advanced Study Institute on Dynamic Modeling and Flow in the Earth and Planets*, Ed. by K. E. Runcorn and D. Stone (Kluwer, Dordrecht, 1993).

64. I. Prigogine, *Introduction to Thermodynamics of Irreversible Processes* (Springfield, Ill., 1955).

65. Y. N. Rabotnov, *A Mechanism of a Long Time Failure, in: Creep Problems in Structural Members* (AN SSSR. 1959) [in Russian].

66. Y. N. Rabotnov, *Mechanics of Deformable Solids* (Nauka, Moscow, 1988) [in Russian].

67. C. I. Renshaw, "On the Relationship between Mechanical and Hydraulic Apertures in Rough-Walled Fractures," J. Geophys. Res. **100**, 24 629–24 636 (1995).

68. C. I. Renshaw, "Influence of Subcritical Fracture Growth on the Connectivity of Fracture Networks," Water Res. Res. **32**, 1519–1530 (1996).

69. J. R. Rice and M. P. Cleary, "Some Basic Stress Diffusion Solutions for Fluid-Saturated Elastic Porous Media with Compressible Constituents," Rev. Geophys. Space Phys. **14**, 227–241 (1976).

70. J. R. Rice, "Fault Stress States, Pore Pressure Distribution, and the Weakness of the San Andreas Fault," in *Fault Mechanics and Transport Properties of Rocks*, Ed. by B. Evans and T. F. Wong (1992), pp. 476–503 (1992).

71. E. L. Robinson, "Effect of Temperature Variation on the Long-Term Rupture Strength of Steels," Trans. Am. Soc. Mech. Eng. **174**, 777–781 (1952).

72. A. M. Rubin, "Tensile Fracture of Rock at High Confining Pressure: Implications for Dike Propagation," J. Geophys. Res. **98**, 15 919–15 935 (1993).

73. L. I. Sedov, "Variational Methods of Constructing Models of Continuous Media," in *Irreversible Aspects of Continuum Mechanics* (Springer, 1968), pp. 17–40.

74. B. Seront, T.-F. Wong, J. S. Caine, et al., "Laboratory Characterization of a Seismogenic Normal Fault System," J. Struct. Geol. **20**, 865–881 (1998).

75. E. Tenthorey, C. H. Scholz, E. Aharonov, and A. Leger, "Precipitation Sealing and Diagenesis 1. Experimental Results," J. Geophys. Res. **103**, 23 951–23 967 (1998).

76. E. Tenthorey, S. F. Cox, and H. F. Todd, "Evolution of Strength Recovery and Permeability during Fluid-Rock Reaction in Experimental Fault Zones," Earth Planet. Sci. Lett. **206**, 161–172 (2003).

77. D. L. Turcotte, W. I. Newman, and R. Shcherbakov, "Micro and Macroscopic Models of Rock Fracture," Geophys. J. Int. **152**, 718–728 (2003).

78. K. C. Valanis, "A Theory of Damage in Brittle Materials," Eng. Fract. Mech. **36**, 403–416 (1990).

79. T.-F. Wong and W. Zhu, "Brittle Faulting and Permeability Evolution: Hydromechanical Measurement, Microstructural Observation, and Network Modeling," in *Faults and Subsurface Fluid Flow in the Shallow Crust (Geophys. Monogr., Vol. 113)*, Ed. by W. C. Haneberg, P. S. Mozley, J. C. Moore, and L. B. Goodwin (AGU, Washington DC, 1999), pp. 83–99.

80. T.-F. Wong, C. David, and W. Zhu, "The Transition from Brittle Faulting to Cataclastic Flow in Porous Sandstones: Mechanical Deformation," J. Geophys. Res. **102**, 3009–3025 (1997).

81. S. Zhang, M. S. Paterson, and S. F. Cox, "Porosity and Permeability Evolution during Hot Isostatic Pressing of Calcite Aggregates," J. Geophys. Res. **99**, 15741–15760 (1994).

82. J. Zhang, T.-F. Wong, and D. M. Davies, "Micromechanics of Pressure-Induced Grain Crushing in Porous Rocks," J. Geophys. Res. **95**, 341–352 (1990).

83. W. Zhu, C. David, and T.-F. Wong, "Network Modeling of Permeability Evolution during Cementation and Hot Isostatic Pressing," J. Geopys. Res. **100**, 15451–15464 (1995).